Signal & Image Processing: An International Journal (SIPIJ) Vol.11, No.3, June 2020

DEMOSAICING MASTCAM IMAGES USING A NEW COLOR FILTER ARRAY

Chiman Kwan and Jude Larkin

Applied Research, LLC, Rockville, Maryland, USA

ABSTRACT

The two mast cameras (Mastcam) act as eyes of the NASA's Mars rover Curiosity. They can work independently or together for near and long range (up to 1 km) rover guidance and rock sample selection. Currently, the Mastcams are using Bayer color filter array (CFA), also known as CFA 1.0, in generating the RGB images. Under normal lighting conditions, CFA 1.0 is sufficient. However, since Mastcam may need to collect images under different lighting conditions such as early morning and sunset hours or sand storm periods, the lighting conditions in those scenarios will be unfavorable. It will be good to investigate a CFA that is robust to various lighting conditions. In the past, we have compared CFA 1.0 and CFA 2.0 for normal and low lighting images. Recently, a new CFA known as CFA 3.0 has been proposed by our team. CFA 3.0 has 75% white pixels, which are believed to be able to enhance the sensitivity of cameras. In this paper, we will first review some past demosaicing results for Mastcams. We will then investigate the performance of CFA 3.0 for Mastcam images in normal lighting conditions. Experiments using actual Mastcam images show that the demosaicing image quality using CFA 3.0 is satisfactory based on objective and subjective evaluations.

KEYWORDS

Mastcam, debayering; demosaicing, color filter array (CFA), RGBW pattern, Bayer pattern, CFA 1.0, CFA2.0, CFA3.0, pansharpening, deep learning

1. INTRODUCTION

The Curiosity rover (Figure 1) has several instruments that are able to characterize the Mars surface. The Alpha Particle X-Ray Spectrometer (APXS) [1] can analyze rock samples and extract compositions of rocks; the Laser Induced Breakdown Spectroscopy (LIBS) [2] can deduce the rock compositions at a distance of 7 m; and Mastcam imagers [3] can perform surface characterization from 1 km away.

Figure 1. Curiosity rover [4].

DOI: 10.5121/sipij.2020.11301

The two Mastcam multispectral imagers have nine bands in each and are separated by 24.2 cm [3]. Figure 2 shows a schematic of Mastcam. The left Mastcam (34 mm focal length) has three times the field of view of the right Mastcam (100 mm focal length). In other words, the right imager has three times higher resolution than that of the left. Stereo image formation and image fusion have been done by combining the left and right bands to form a 12-band image cube [5]-[7]. The current practice is to downsample the right images to the resolution of the left, avoiding artifacts due to Bayer pattern and also lossy JPEG compression [8]. This practice has practical merits, but may restrict the potential of Mastcams. First, downsampling the right images will throw away those high spatial resolution pixels in the right bands. Second, the lower resolution of the current stereo images may degrade the augmented reality or virtual reality experience of users. If one can apply some advanced pansharpening algorithms to the left bands, then one can have 12 bands of high resolution image cube for stereo vision and image fusion.

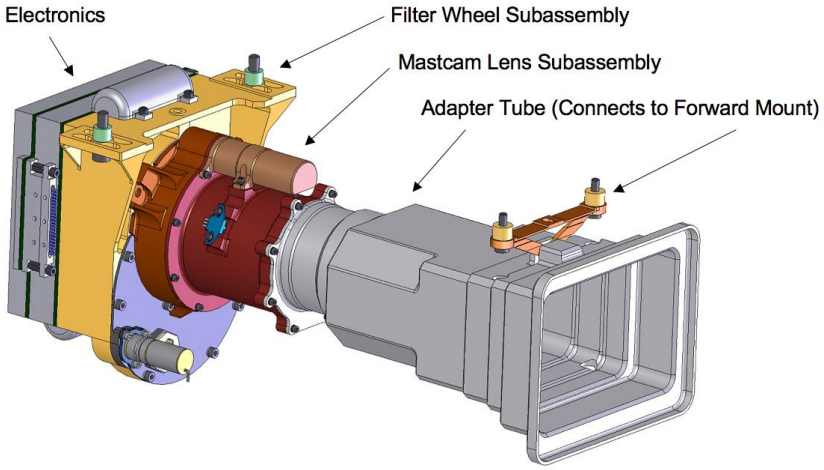

Figure 2. The Mastcam imager [9].

Out of the nine bands, the RGB bands are generated by using a Bayer pattern. Bayer pattern was invented in 1976 [10]. One example is shown in Figure 3 (a). For demosaicing the RGB bands, the current Mastcam uses Malvar-He-Cutler (MHC) algorithm [11], which was published in 2004, due to its simplicity and computational efficiency. In Bell's paper [3], Directional Linear Minimum Mean Square-Error Estimation (DLMMSE) [12] was also evaluated.

After the successful commercial use of Bayer pattern, Kodak researchers invented CFA 2.0 (Figure 3 (b)) [13]-[15]. Numerous other CFA patterns have been invented in the past few decades [16]-[18]. Recently, we proposed a simple CFA pattern [19] in which the RGB pixels are evenly distributed. In particular, as shown in Figure 3 (c), each 4x4 block has 75% or 12 white pixels, 12.5% or two green pixels, 6.25% or one red and blue pixels. We call this CFA pattern the CFA 3.0. In addition to simplicity, CFA 3.0 has one distinct advantage in that some of the demosaicing algorithms for CFA 2.0 can be applied with little modifications.

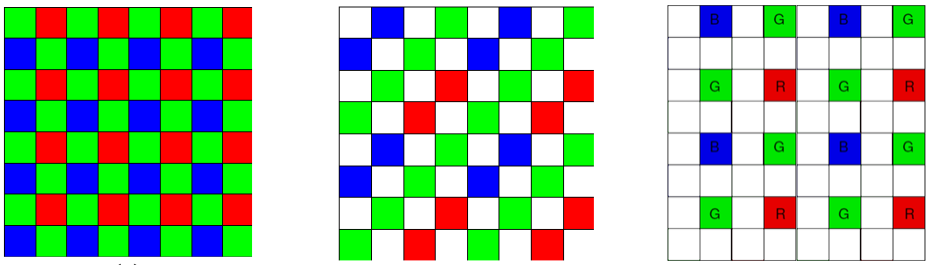

(a) (b) (c)

Figure 3. Three CFA patterns. (a) CFA 1.0; (b) CFA 2.0; (c) CFA 3.0.

Although the Bayer pattern works well under normal lighting conditions for Mastcam, Mastcam may also need to collect data under unfavorable lighting conditions such as early morning and sunset hours or sand storm periods. It will be good to investigate a CFA that is robust to various lighting conditions. In the past, we have compared CFA 1.0 and CFA 2.0 for normal and low lighting images [20]. CFA 2.0 was observed to perform better than CFA 1.0 under dark environments. Our recently proposed CFA 3.0 has 75% white pixels may be a good candidate to meet the diverse lighting conditions of Mastcam. In this paper, we will first review some past demosaicing results for Mastcams using CFA 1.0. We will then investigate the performance of CFA 3.0 for Mastcam images in normal lighting conditions. We have not worked on Mastcam images that were collected in low lighting conditions yet and will plan to continue that effort in the near future. Experiments using actual Mastcam images show that the demosaicing quality using CFA 3.0 is satisfactory based on objective and subjective evaluations.

The rest of this paper is organized as follows. In Section 2, we will briefly review those representative demosaicing methods for CFA 1.0 and CFA 3.0. In Section 3, we will first present some demosaicing results for CFA 1.0. We will then present those new results for CFA 3.0. Both objective and subjective results will be presented. Finally, Section 4 concludes the paper with some remarks and future directions.

2. DEMOSAICING METHODS

2.1. Methods for CFA 1.0

The following algorithms for CFA 1.0 were evaluated in our experiments and they are briefly summarized below:

- Malvar–He–Cutler (MHC) [11].
- Bilinear [11].
- Directional Linear Minimum Mean Square-Error Estimation (DLMMSE) [12].
- Linear Directional Interpolation and Nonlocal Adaptive Thresholding (LDI-NAT) [21].
- Lu and Tan Interpolation (LT) [22].
- Adaptive Frequency Domain (AFD) [23].
- Alternate Projection (AP) [24].
- Primary-Consistent Soft-Decision (PCSD) [25].
- Fusion using 3 best (F3) [26].
- Alpha Trimmed Mean Filtering (ATMF) [26][27].
- Demosaicnet (DEMONET) [28].

2.2. Methods for CFA 3.0

Details of the demosaicing algorithms for CFA 3.0 can be found in a companion paper [19]. We skip the details here. The Baseline method refers to the demosaicing of the low resolution color Bayer pattern in Figure 3 (c). The Standard method is the method shown in Figure 2 of [19]. The other methods involve the use of pansharpening methods, including Principal Component Analysis (PCA) [29], Smoothing Filter-based Intensity Modulation (SFIM) [30], Modulation Transfer Function Generalized Laplacian Pyramid (MTF-GLP) [31], MTF-GLP with High Pass Modulation (MTF-GLP-HPM) [32], Gram Schmidt (GS) [33], GS Adaptive (GSA) [34], Guided Filter PCA (GFPCA) [35], PRACS [36] and hybrid color mapping (HCM) [37]-[40]. The pansharpening based algorithms can be illustrated in Figure 4 below.

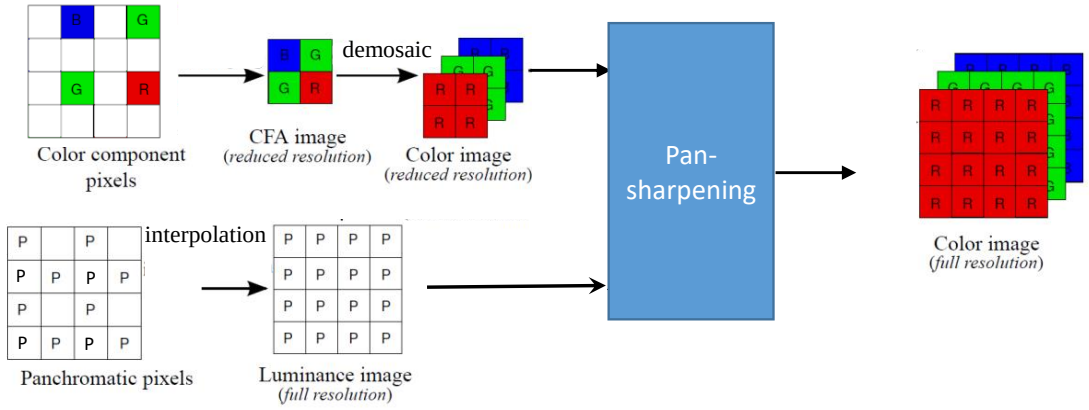

Figure 4. A pan-sharpening approach for CFA 3.0.

3. RESULTS

3.1. Data

From the NASA's Planetary Data System (PDS), we have retrieved 31 actual Mastcam images, which were losslessly compressed and saved in Bayer pattern. Figure 5 and Figure 6 show 16 left Mastcam images and 15 right Mastcam images, respectively. All of the debayered images using various algorithms have been subjectively evaluated.

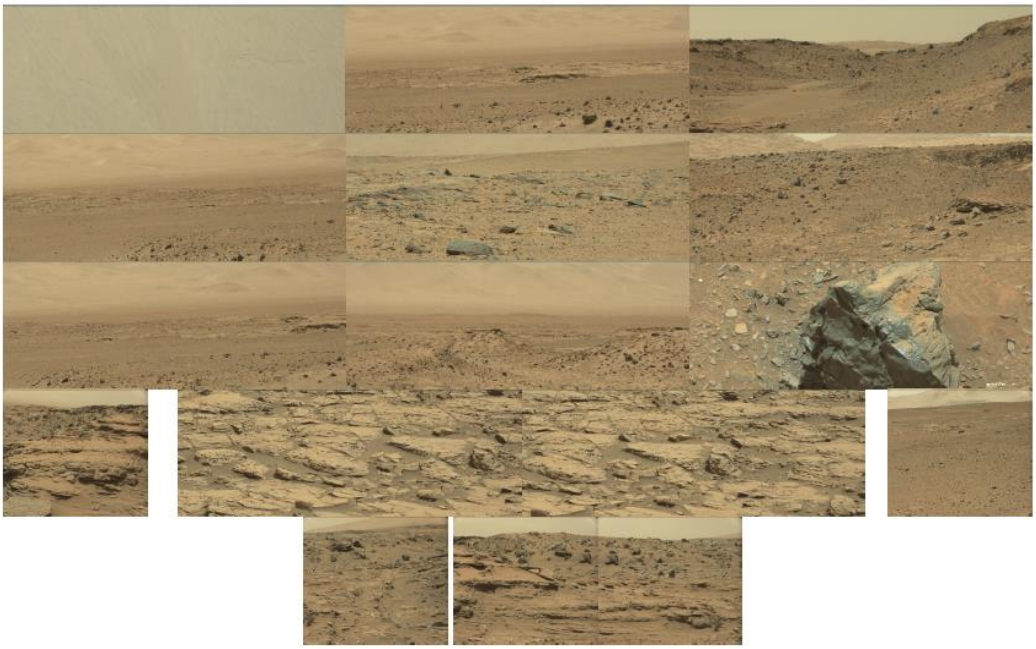

Figure 5. Images from the left Mastcam.

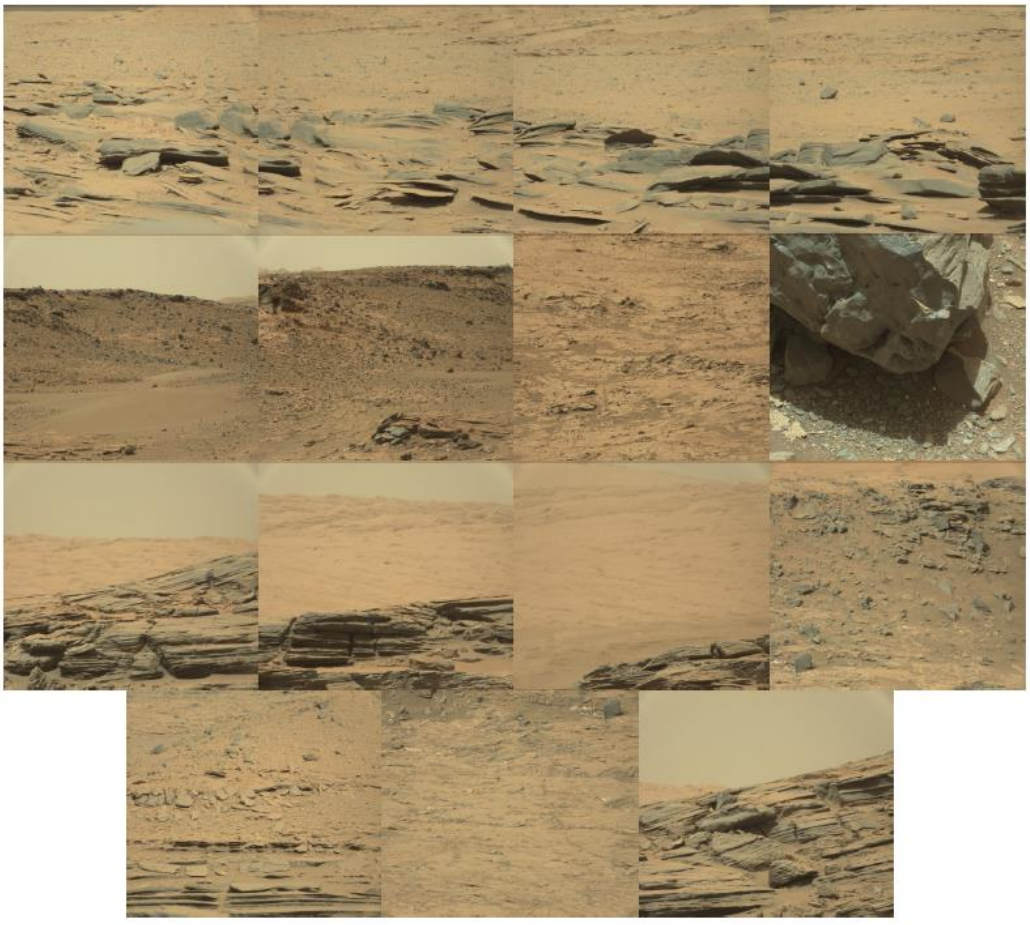

Figure 6. Images from the right Mastcam.

3.2. Performance metrics

We have used the following metrics to evaluate different methods:

- Peak Signal-to-Noise Ratio (PSNR) [41]
  Separate PSNRs in dBs are computed for each band. A combined PSNR is the average of the PSNRs of the individual bands. Higher PSNR values imply higher image quality.
- Structural SIMilarity (SSIM)
  In [42], SSIM was defined to measure the closeness between two images. An SSIM value of 1 means that the two images are the same.
- Human Visual System (HVS) metric
  Details of HVS metric in dB can be found in [43].
- HVSm (HVS with masking) [44]
  Similar to HVS, HVS incorporates the visual masking effects in computing the metrics.
- CIELAB
  We also used CIELAB [45] for assessing demosaicing performance in our experiments.
- Naturalness Image Quality Evaluator (NIQE) [46][47]
  The ground truth RGB images are not available to use so demosaiced images are used as the ground truth. These demosaiced images contain some loss so a new metric was used to help evaluate the results. NIQE is used to evaluate the quality of images without the presence of a reference image. A model was trained using six sharp images from the right dataset. This model was used in generating the scores. The lower the score the better quality the image is.

3.3. CFA 1.0 Results

We briefly summarize our earlier results for demosaicing CFA 1.0. More results can be found in [48][49].

3.3.1. Comparison of Demosaiced Left Images

Figure 7 shows a visual comparison of demosaiced images from different methods. One can see that DEMONET has the lowest distortion in terms of color integrity and zipper effects. Although the MHC algorithm was developed in 2004, it still performed quite well. This is a surprise in our research, as MHC is so simple and yet its performance is not bad for this NASA application.

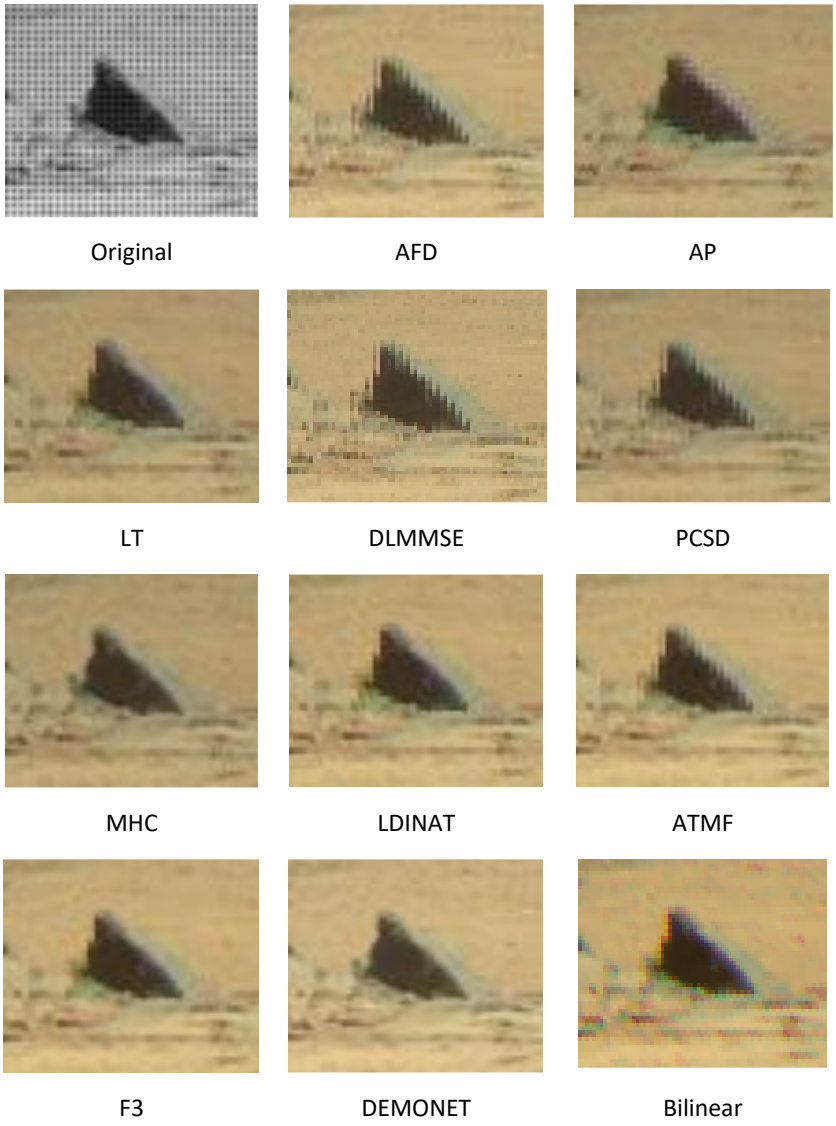

Figure 7. Visual comparison of demosaiced images of different algorithms for a left Mastcam image 5.

3.3.2. Comparison of Demosaiced Right Images

We can see that DEMONET outperforms all others. The second best method is still the MHC. Figure 8 shows a visual comparison of demosaiced images from different methods. One can see that DEMONET has the lowest distortion in terms of color integrity and zipper effects.

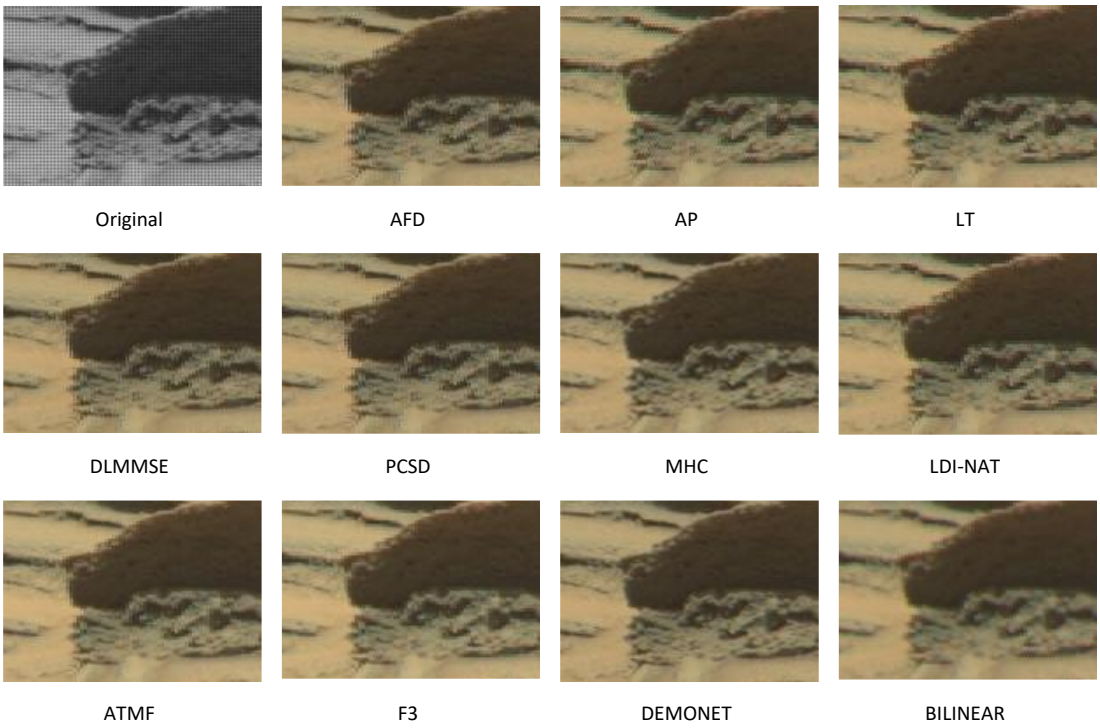

Figure 8. Visual comparison of demosaiced images of different algorithms for a right Mastcam image 3.

3.4. CFA 3.0 Results

We have evaluated 11 methods in our experiments for CFA 3.0. In all the methods, the reduced resolution images were demosaiced using LDI-NAT [21]. The panchromatic bands were also interpolated using LDI-NAT [21]. The pansharpening methods are mentioned before.

Table 1 shows the metrics for the left images and Table 2 shows the metrics for the right images. There are six metrics in each table. From those tables, it appears that GFPCA yielded the best performance and the Baseline method had the worst performance. Figure 9 and Figure 11 show the averaged performance metrics of the demosaiced left and right images, respectively. From those two figures on the averaged results, we can see that GFPCA has the best performance except SSIM. Based on visual inspection of those demosaiced images shown in Figure 10 and Figure 12, it is indeed very difficult to tell which method is better than others. This means that all methods work quite well.

Table 1. Performance metrics of 20 left Mastcam images. Bold numbers indicate the best methods of each row.

Image		Baseline	Standard	GSA	HCM	SFIM	PCA	GFPCA	GLP	HPM	GS	PRACS	Best Score
Img1	PSNR	33.051	36.321	36.206	35.909	35.599	34.736	**36.908**	35.552	35.532	34.788	35.833	36.908
	Cielab	2.138	1.712	1.748	1.792	1.789	1.922	**1.385**	1.802	1.801	1.895	1.858	1.385
	SSIM	0.820	**0.934**	0.930	0.924	0.923	0.902	0.922	0.921	0.920	0.906	0.911	0.934
	HVS	29.993	30.288	30.283	30.117	30.149	30.315	**34.076**	30.180	30.167	29.895	30.287	34.076
	HVSm	31.970	32.114	32.169	32.082	32.107	32.127	**36.982**	32.109	32.106	31.628	32.145	36.982
	NIQE	10.857	5.673	5.709	5.626	5.925	5.567	**5.355**	5.865	5.853	5.564	5.796	5.355
Img2	PSNR	30.322	33.465	33.398	33.015	32.799	32.502	**34.682**	32.766	32.742	32.581	33.132	34.682
	Cielab	3.586	2.894	2.932	3.036	2.999	3.141	**2.208**	3.035	3.017	3.108	3.085	2.208
	SSIM	0.832	**0.939**	0.937	0.928	0.930	0.920	0.933	0.929	0.928	0.922	0.922	0.939
	HVS	26.939	27.260	27.259	27.038	27.123	27.292	**31.764**	27.161	27.138	27.069	27.235	31.764
	HVSm	28.817	29.000	29.032	28.920	28.969	29.031	**34.685**	28.978	28.965	28.771	28.989	34.685
	NIQE	10.212	6.222	6.420	6.440	6.246	6.226	6.175	**6.111**	6.118	6.256	6.384	6.111
Img3	PSNR	46.569	**48.257**	48.195	47.973	48.034	45.205	48.052	47.837	47.805	43.771	47.905	48.257
	Cielab	0.492	0.442	0.446	0.453	0.446	0.569	**0.434**	0.457	0.457	0.631	0.463	0.434

	SSIM	0.668	**0.824**	0.822	0.816	0.817	0.728	0.735	0.803	0.802	0.710	0.787	0.824
	HVS	42.948	43.057	43.016	42.851	42.879	42.179	**43.941**	42.932	42.879	41.736	43.025	43.941
	HVSm	44.745	44.800	44.782	44.672	44.696	43.639	**45.680**	44.742	44.704	43.214	44.791	45.680
	NIQE	15.762	11.173	10.992	11.530	**10.559**	13.984	12.115	10.837	10.866	13.355	11.353	10.559
Img4	PSNR	43.375	45.148	44.920	44.844	44.684	41.120	**46.214**	44.571	44.549	41.901	44.692	46.214
	Cielab	0.802	0.716	0.738	0.743	0.738	0.944	**0.614**	0.744	0.746	0.864	0.764	0.614
	SSIM	0.823	0.903	0.894	0.892	0.894	0.819	**0.903**	0.890	0.889	0.837	0.874	0.903
	HVS	38.364	38.487	38.271	38.274	38.188	36.639	**40.864**	38.245	38.213	36.880	38.378	40.864
	HVSm	40.001	40.086	39.993	39.975	39.945	37.776	**42.765**	39.987	39.965	38.154	40.038	42.765
	NIQE	14.340	9.341	**9.215**	9.402	9.924	9.723	9.354	9.898	9.845	9.549	9.702	9.215
Img5	PSNR	27.229	29.957	29.755	29.323	29.346	29.250	**31.642**	29.349	29.302	29.504	29.759	31.642
	Cielab	6.028	5.047	5.197	5.433	5.181	5.450	**3.654**	5.269	5.209	5.310	5.357	3.654
	SSIM	0.829	0.924	0.922	0.903	0.915	0.898	**0.934**	0.915	0.915	0.904	0.906	0.934
	HVS	23.365	23.501	23.279	23.239	23.460	23.919	**28.898**	23.487	23.491	23.524	23.471	28.898
	HVSm	25.371	25.419	25.266	25.406	25.513	25.941	**31.830**	25.510	25.521	25.461	25.404	31.830
	NIQE	11.151	**7.949**	8.082	7.977	8.033	8.051	7.967	8.101	8.124	7.995	8.180	7.949
Img6	PSNR	34.028	36.814	36.661	36.371	36.205	36.105	**37.139**	36.226	36.167	36.464	36.400	37.139
	Cielab	2.188	1.791	1.822	1.863	1.888	2.654	**1.509**	1.883	1.899	2.523	1.894	1.509
	SSIM	0.787	**0.909**	0.899	0.893	0.893	0.846	0.881	0.896	0.891	0.851	0.887	0.909
	HVS	30.706	31.036	31.042	30.932	31.018	31.369	**33.300**	31.082	31.088	30.981	31.057	33.300
	HVSm	32.779	32.970	33.097	33.059	33.155	33.460	**35.661**	33.186	33.215	32.988	33.023	35.661
	NIQE	10.572	6.080	6.079	6.048	6.002	6.402	6.135	6.029	6.009	6.113	**5.962**	5.962
Img7	PSNR	34.028	36.814	36.661	36.371	36.205	36.105	**37.139**	36.226	36.167	36.464	36.400	37.139
	Cielab	2.188	1.791	1.822	1.863	1.888	2.654	**1.509**	1.883	1.899	2.523	1.894	1.509
	SSIM	0.787	**0.909**	0.899	0.893	0.893	0.846	0.881	0.896	0.891	0.851	0.887	0.909
	HVS	30.706	31.036	31.042	30.932	31.018	31.369	**33.300**	31.082	31.088	30.981	31.057	33.300
	HVSm	32.779	32.970	33.097	33.059	33.155	33.460	**35.661**	33.186	33.215	32.988	33.023	35.661
	NIQE	10.572	6.080	6.079	6.048	6.002	6.402	6.135	6.029	6.009	6.113	**5.962**	5.962
Img8	PSNR	33.211	35.514	34.523	34.943	34.792	34.517	37.414	34.744	34.723	35.017	35.097	37.414
	Cielab	2.516	2.147	2.346	2.301	2.271	2.367	**1.559**	2.289	2.285	2.273	2.308	1.559
	SSIM	0.857	0.930	0.923	0.914	0.921	0.907	**0.942**	0.920	0.920	0.914	0.917	0.942
	HVS	28.415	28.693	28.211	28.243	28.434	29.155	**33.210**	28.482	28.468	28.477	28.397	33.210
	HVSm	30.407	30.626	30.278	30.358	30.541	31.297	**35.779**	30.567	30.561	30.467	30.344	35.779
	NIQE	10.361	6.860	6.994	6.809	6.980	6.803	**6.508**	6.948	6.946	6.840	7.151	6.508
Img9	PSNR	37.094	39.615	39.410	38.953	38.991	37.482	**40.758**	38.962	38.918	38.113	38.956	40.758
	Cielab	1.462	1.248	1.282	1.329	1.282	1.488	**1.051**	1.293	1.292	1.395	1.362	1.051
	SSIM	0.798	**0.903**	0.896	0.886	0.895	0.845	0.888	0.893	0.892	0.866	0.868	0.903
	HVS	32.858	33.175	33.024	32.652	32.806	33.139	**36.365**	32.928	32.849	32.575	33.010	36.365
	HVSm	34.804	35.031	34.976	34.714	34.865	34.977	**38.411**	34.936	34.895	34.326	34.936	38.411
	NIQE	10.461	6.550	6.520	6.494	6.590	**6.437**	6.441	6.578	6.661	6.697	6.733	6.437
Img10	PSNR	31.316	34.227	32.424	33.584	33.561	33.303	**35.358**	33.547	33.525	33.814	33.234	35.358
	Cielab	3.074	2.508	3.023	2.680	2.616	2.756	**2.014**	2.644	2.627	2.651	2.863	2.014
	SSIM	0.767	**0.909**	0.894	0.888	0.897	0.882	0.887	0.896	0.896	0.891	0.873	0.909
	HVS	27.134	27.327	26.720	26.906	27.089	27.782	**31.566**	27.158	27.123	27.172	27.028	31.566
	HVSm	28.979	29.055	28.587	28.816	28.974	29.691	**34.048**	29.008	28.986	28.947	28.811	34.048
	NIQE	10.035	5.588	5.579	5.696	5.578	5.563	**5.113**	5.648	5.672	5.738	5.401	5.113
Img11	PSNR	31.316	34.227	32.424	33.584	33.561	33.303	**35.358**	33.547	33.525	33.814	33.234	35.358
	Cielab	3.074	2.508	3.023	2.680	2.616	2.756	**2.014**	2.644	2.627	2.651	2.863	2.014
	SSIM	0.767	**0.909**	0.894	0.888	0.897	0.882	0.887	0.896	0.896	0.891	0.873	0.909
	HVS	27.134	27.327	26.720	26.906	27.089	27.782	**31.566**	27.158	27.123	27.172	27.028	31.566
	HVSm	28.979	29.055	28.587	28.816	28.974	29.691	**34.048**	29.008	28.986	28.947	28.811	34.048
	NIQE	10.035	5.588	5.579	5.696	5.578	5.563	**5.113**	5.648	5.672	5.738	5.401	5.113
Img12	PSNR	28.812	31.744	31.544	31.024	31.167	30.952	**32.667**	31.132	31.104	31.270	31.258	32.667
	Cielab	4.468	3.651	3.824	4.004	3.756	4.042	**2.870**	3.803	3.783	3.915	4.013	2.870
	SSIM	0.810	**0.920**	0.905	0.894	0.913	0.883	0.914	0.912	0.911	0.892	0.890	0.920
	HVS	25.381	25.540	25.436	25.216	25.497	25.899	**31.262**	25.514	25.530	25.552	25.551	31.262
	HVSm	27.521	27.571	27.545	27.530	27.683	28.041	**34.446**	27.664	27.691	27.615	27.610	34.446
	NIQE	9.404	6.324	6.637	6.267	6.403	6.687	**6.090**	6.438	6.439	6.607	6.701	6.090
Img13	PSNR	31.085	**34.261**	33.673	33.542	33.498	33.316	33.993	33.538	33.506	33.582	33.534	34.261
	Cielab	3.462	2.724	2.910	2.945	2.919	3.020	**2.318**	2.920	2.926	2.944	3.022	2.318
	SSIM	0.770	**0.920**	0.910	0.899	0.901	0.886	0.871	0.900	0.901	0.891	0.887	0.920
	HVS	28.654	29.121	28.643	28.708	28.741	29.470	**32.899**	28.877	28.860	28.834	28.909	32.899
	HVSm	30.723	31.032	30.790	30.901	30.903	31.675	**35.862**	31.011	31.014	30.861	30.865	35.862
	NIQE	11.079	8.292	8.380	8.277	**8.149**	8.433	8.314	8.211	8.169	8.361	8.347	8.149
Img14	PSNR	36.789	39.326	39.032	38.711	38.590	36.243	**40.380**	38.533	38.488	37.448	38.570	40.380
	Cielab	1.617	1.377	1.431	1.467	1.427	1.793	**1.178**	1.438	1.439	1.572	1.520	1.178
	SSIM	0.823	**0.917**	0.906	0.900	0.907	0.839	0.910	0.905	0.903	0.878	0.879	0.917
	HVS	32.281	32.631	32.368	32.128	32.132	32.154	**35.239**	32.263	32.180	31.778	32.405	35.239
	HVSm	34.219	34.492	34.387	34.196	34.249	33.833	**37.089**	34.330	34.286	33.488	34.354	37.089
	NIQE	11.555	5.873	5.744	5.845	6.036	5.835	**5.471**	6.047	6.034	5.962	6.299	5.471
Img15	PSNR	35.903	38.697	38.367	38.087	37.955	36.338	**39.572**	37.884	37.864	36.904	37.888	39.572
	Cielab	1.835	1.512	1.583	1.618	1.579	1.838	**1.285**	1.594	1.592	1.724	1.698	1.285
	SSIM	0.802	**0.922**	0.909	0.904	0.909	0.863	0.898	0.908	0.907	0.885	0.876	0.922
	HVS	31.685	32.024	31.758	31.573	31.611	32.081	**34.553**	31.690	31.644	31.160	31.829	34.553
	HVSm	33.625	33.865	33.778	33.619	33.705	33.983	**36.501**	33.751	33.726	32.880	33.765	36.501
	NIQE	10.912	5.441	5.380	5.426	5.452	5.321	**5.311**	5.515	5.533	5.520	5.701	5.311
Img16	PSNR	32.678	**36.192**	35.892	35.461	35.442	34.400	35.789	35.433	35.376	34.784	35.329	36.192
	Cielab	2.734	2.155	2.243	2.342	2.253	2.559	**1.916**	2.267	2.268	2.470	2.441	1.916
	SSIM	0.771	**0.924**	0.913	0.901	0.910	0.877	0.880	0.909	0.907	0.889	0.876	0.924
	HVS	29.543	29.951	29.707	29.398	29.541	30.165	**33.162**	29.590	29.533	29.501	29.776	33.162
	HVSm	31.539	31.816	31.742	31.554	31.639	32.234	**35.697**	31.649	31.609	31.381	31.724	35.697
	NIQE	11.595	11.071	11.664	11.526	10.373	10.914	10.217	10.248	**10.132**	11.528	10.505	10.132
Img17	PSNR	35.604	38.686	34.235	38.125	38.039	37.533	**38.992**	37.994	37.985	37.769	36.722	38.992
	Cielab	1.900	1.542	2.261	1.648	1.607	1.722	1.323	1.618	1.617	1.680	1.859	1.323
	SSIM	0.802	**0.922**	0.875	0.904	0.911	0.892	0.903	0.910	0.909	0.898	0.887	0.922
	HVS	32.258	32.557	31.128	32.244	32.396	32.687	**35.583**	32.436	32.430	32.328	32.066	35.583
	HVSm	34.224	34.401	33.048	34.290	34.382	34.580	**37.884**	34.396	34.393	34.152	33.924	37.884
	NIQE	10.550	5.424	5.726	5.338	5.574	5.485	**5.258**	5.630	5.627	5.505	5.886	5.258

Img18	PSNR	33.105	36.287	33.758	35.633	35.619	35.147	**36.869**	35.580	35.569	35.426	35.093	36.869
	Cielab	2.564	2.053	2.547	2.210	2.145	2.283	**1.670**	2.167	2.159	2.222	2.353	1.670
	SSIM	0.787	**0.918**	0.891	0.898	0.906	0.884	0.901	0.905	0.905	0.891	0.884	0.918
	HVS	29.615	29.997	29.226	29.600	29.852	30.086	**33.640**	29.901	29.895	29.718	29.686	33.640
	HVSm	31.633	31.873	31.225	31.705	31.871	32.004	**36.295**	31.898	31.896	31.568	31.624	36.295
	NIQE	9.985	5.862	6.323	5.910	**5.811**	6.083	5.915	5.972	5.984	6.085	6.205	5.811
Img19	PSNR	34.582	37.472	34.331	36.872	36.812	36.204	**38.740**	36.747	36.739	36.681	35.974	38.740
	Cielab	2.113	1.744	2.330	1.862	1.814	1.959	1.393	1.835	1.826	1.876	2.040	1.393
	SSIM	0.793	**0.912**	0.873	0.892	0.901	0.876	0.905	0.899	0.899	0.887	0.874	0.912
	HVS	30.245	30.507	29.687	30.116	30.388	30.688	**34.145**	30.418	30.409	30.266	30.179	34.145
	HVSm	32.094	32.245	31.550	32.055	32.271	32.495	**36.372**	32.284	32.277	32.000	31.982	36.372
	NIQE	9.780	4.121	4.562	4.145	**3.934**	4.244	3.937	4.158	4.157	4.304	4.504	3.934
Img20	PSNR	32.759	35.754	33.634	35.033	35.109	34.822	36.809	35.057	35.041	35.100	34.634	36.809
	Cielab	2.733	2.226	2.720	2.405	2.310	2.444	**1.767**	2.340	2.326	2.383	2.544	1.767
	SSIM	0.795	**0.918**	0.899	0.897	0.908	0.891	0.909	0.907	0.906	0.897	0.890	0.918
	HVS	28.965	29.327	28.681	28.783	29.136	29.397	**33.120**	29.185	29.166	29.099	28.992	33.120
	HVSm	30.985	31.238	30.673	30.925	31.169	31.343	**35.566**	31.196	31.181	30.986	30.945	35.566
	NIQE	9.998	5.158	5.476	5.247	5.106	5.313	**4.767**	5.286	5.308	5.339	5.405	4.767
Average	PSNR	34.143	36.939	35.952	36.368	36.300	35.429	**37.724**	36.261	36.231	35.760	36.182	37.724
	Cielab	2.549	2.090	2.311	2.234	2.176	2.418	**1.683**	2.196	2.190	2.330	2.310	1.683
	SSIM	0.794	**0.913**	0.900	0.896	0.902	0.868	0.894	0.900	0.899	0.877	0.882	0.913
	HVS	30.359	30.642	30.275	30.293	30.427	30.678	**34.123**	30.488	30.464	30.235	30.468	34.123
	HVSm	32.310	32.483	32.230	32.333	32.438	32.564	**36.563**	32.470	32.460	32.041	32.355	36.563
	NIQE	10.961	6.734	6.857	6.787	6.713	6.952	**6.585**	6.760	6.758	6.958	6.879	6.585

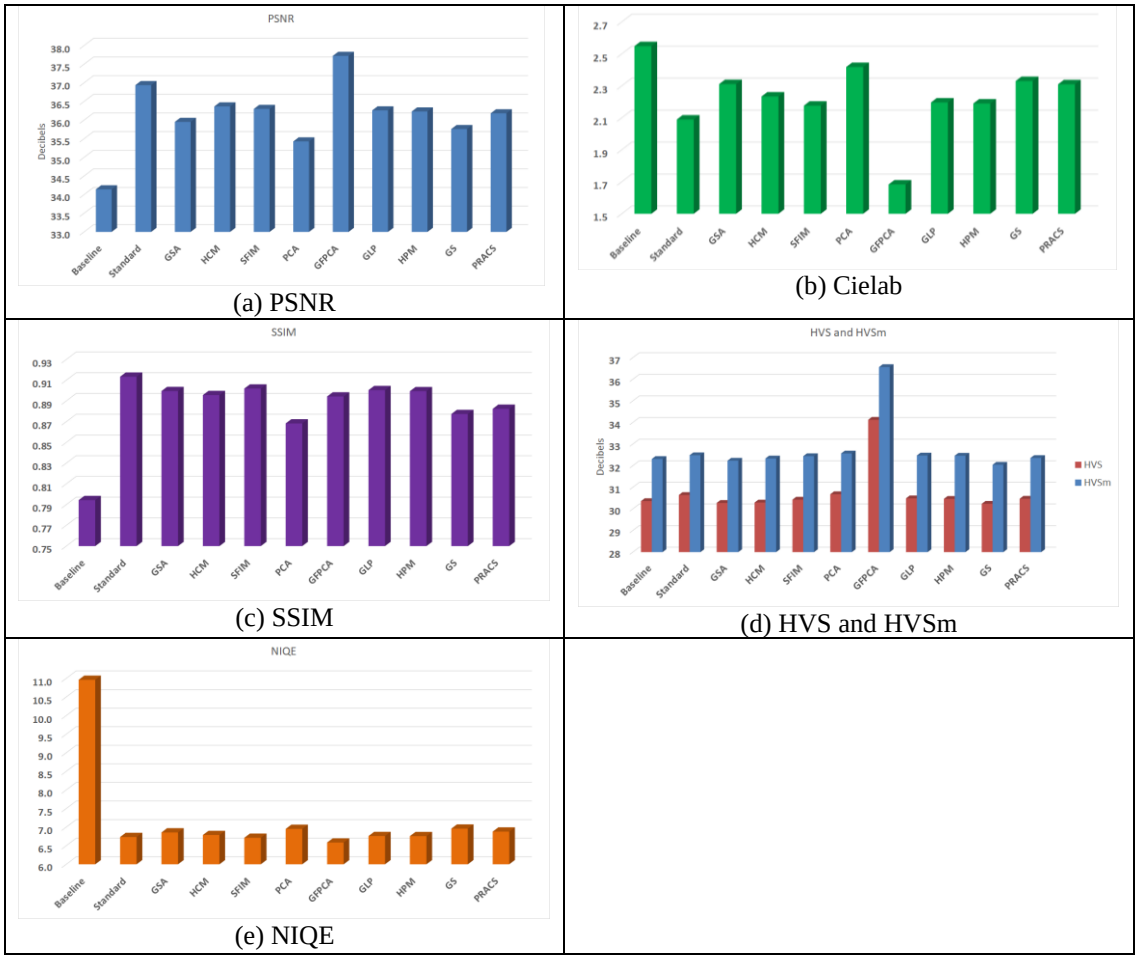

Figure 9. Averaged performance metrics for demosaicing results of left Mastcam images.

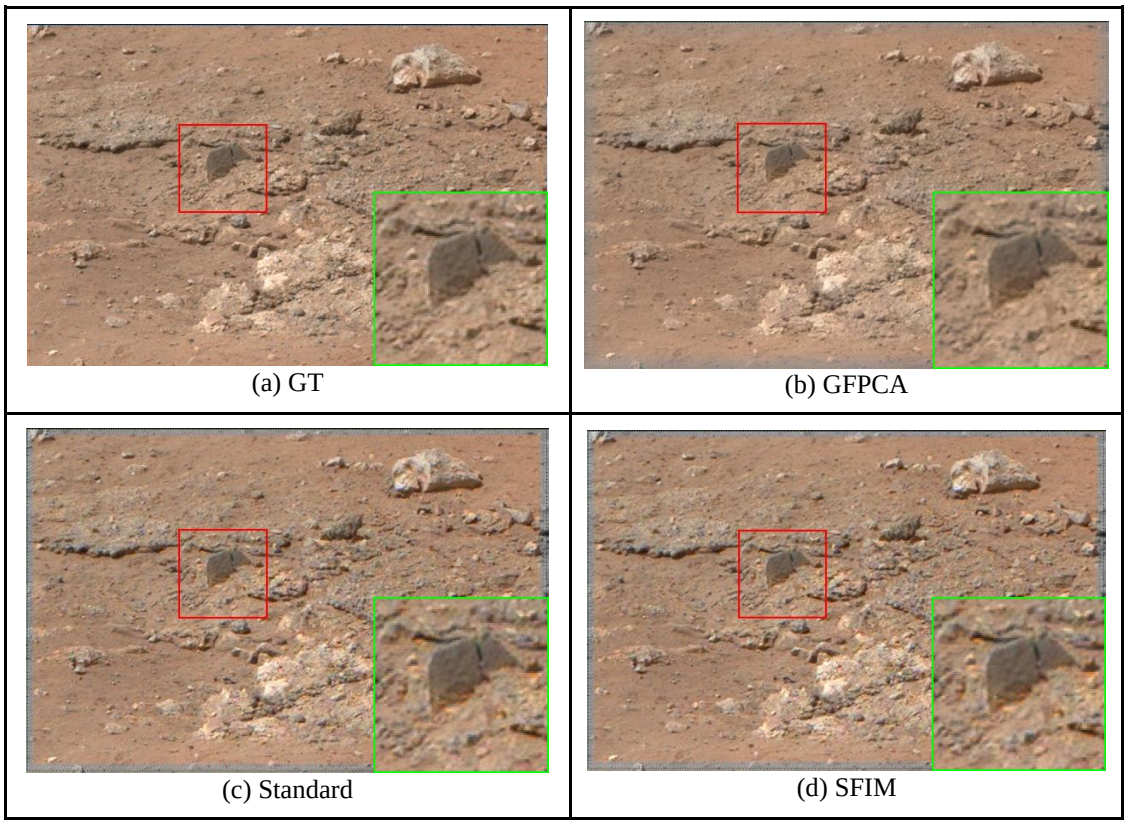

Figure 10. Visual comparison of the ground truth and selected demosaiced images for left Mastcam.

Table 2. Performance metrics of 20 right Mastcam images. Bold numbers indicate the best methods of each row.

Image		Baseline	Standard	GSA	HCM	SFIM	PCA	GFPCA	GLP	HPM	GS	PRACS	Best Score
Img1	PSNR	33.509	36.419	36.398	36.078	35.802	35.621	**37.683**	35.728	35.734	35.736	36.172	37.683
	Cielab	2.011	1.657	1.676	1.729	1.717	1.775	**1.296**	1.732	1.728	1.750	1.751	1.296
	SSIM	0.835	**0.936**	0.934	0.926	0.928	0.920	0.933	0.927	0.927	0.923	0.920	0.936
	HVS	29.787	29.843	30.006	29.836	29.918	30.076	**33.819**	29.937	29.936	29.821	30.000	33.819
	HVSm	31.665	31.615	31.797	31.721	31.780	31.845	**36.483**	31.776	31.777	31.544	31.774	36.483
	NIQE	10.350	5.477	5.495	5.455	5.340	5.506	**5.062**	5.493	5.494	5.515	5.464	5.062
Img2	PSNR	31.714	34.568	34.520	34.161	33.816	34.154	**36.479**	33.752	33.747	34.269	34.386	36.479
	Cielab	3.045	2.543	2.570	2.664	2.645	2.666	**1.854**	2.678	2.662	2.633	2.661	1.854
	SSIM	0.860	0.943	0.941	0.932	0.936	0.933	**0.949**	0.936	0.935	0.935	0.932	0.949
	HVS	27.585	27.816	27.838	27.639	27.747	27.928	**32.254**	27.782	27.765	27.749	27.822	32.254
	HVSm	29.406	29.528	29.570	29.473	29.551	29.655	**35.033**	29.560	29.547	29.446	29.537	35.033
	NIQE	10.158	5.931	5.971	5.895	6.045	5.918	**5.533**	6.177	6.191	5.916	6.024	5.533
Img3	PSNR	48.115	**49.657**	49.547	49.518	49.520	42.835	49.377	49.228	49.234	44.675	49.465	49.657
	Cielab	0.435	0.395	0.399	0.401	0.398	0.735	**0.389**	0.410	0.409	0.596	0.403	0.389
	SSIM	0.655	**0.819**	0.812	0.812	0.815	0.674	0.732	0.799	0.799	0.716	0.787	0.819
	HVS	44.412	44.582	44.512	44.547	44.580	44.006	**45.482**	44.520	44.525	44.146	44.490	45.482
	HVSm	45.970	46.074	46.020	46.072	46.084	45.770	47.219	46.051	46.057	45.820	46.010	47.219
	NIQE	17.458	8.030	7.948	7.852	7.665	11.985	8.618	7.638	**7.633**	10.379	9.358	7.633
Img4	PSNR	47.105	48.249	48.109	48.068	48.030	44.755	**48.870**	47.861	47.855	45.558	47.974	48.870
	Cielab	0.537	0.501	0.509	0.511	0.508	0.647	**0.466**	0.517	0.517	0.600	0.518	0.466
	SSIM	0.761	**0.857**	0.846	0.847	0.849	0.777	0.850	0.841	0.841	0.794	0.825	0.857
	HVS	42.003	42.131	42.042	42.020	42.054	39.769	**43.512**	42.055	42.045	40.231	42.096	43.512
	HVSm	43.411	43.496	43.487	43.441	43.512	40.674	**45.107**	43.526	43.521	41.272	43.495	45.107
	NIQE	17.285	7.288	6.932	7.055	**6.529**	7.333	7.716	6.635	6.613	7.577	8.036	6.529
Img5	PSNR	30.906	33.120	33.122	32.607	32.457	32.969	**36.097**	32.377	32.362	33.099	33.016	36.097
	Cielab	3.949	3.470	3.487	3.706	3.544	3.596	**2.346**	3.601	3.573	3.541	3.604	2.346
	SSIM	0.862	0.931	0.930	0.911	0.927	0.921	**0.953**	0.926	0.926	0.924	0.918	0.953
	HVS	25.608	25.739	25.849	25.473	25.781	25.943	**30.982**	25.796	25.797	25.822	25.806	30.982
	HVSm	27.423	27.489	27.622	27.415	27.600	27.720	**33.403**	27.596	27.600	27.581	27.562	33.403
	NIQE	10.042	5.733	5.755	5.761	5.836	5.800	**5.464**	5.824	5.813	5.753	5.919	5.464
Img6	PSNR	38.249	39.903	39.842	39.596	39.421	38.151	**40.726**	39.330	39.342	39.358	39.647	40.726
	Cielab	1.412	1.282	1.296	1.326	1.317	1.470	**1.137**	1.327	1.325	1.335	1.336	1.137
	SSIM	0.838	**0.911**	0.907	0.900	0.906	0.877	0.900	0.904	0.904	0.897	0.890	0.911
	HVS	32.422	32.604	32.610	32.525	32.658	32.367	**33.126**	32.712	32.698	32.266	32.595	33.126

	HVSm	33.987	34.109	34.152	34.123	34.283	33.821	**34.488**	34.313	34.318	33.736	34.124	34.488
	NIQE	11.233	6.520	6.488	6.448	6.619	7.015	**6.395**	6.687	6.669	6.690	6.918	6.395
Img7	PSNR	36.218	38.266	38.212	37.849	37.633	37.702	**40.270**	37.524	37.541	38.053	38.113	40.270
	Cielab	1.851	1.634	1.651	1.708	1.698	1.732	**1.257**	1.718	1.711	1.692	1.694	1.257
	SSIM	0.865	0.929	0.927	0.917	0.923	0.917	**0.939**	0.922	0.922	0.921	0.918	0.939
	HVS	30.802	31.085	31.082	30.946	31.130	31.269	**33.635**	31.173	31.179	30.966	31.044	33.635
	HVSm	32.541	32.750	32.789	32.758	32.910	32.987	**35.548**	32.934	32.952	32.641	32.721	35.548
	NIQE	12.410	7.342	7.313	**7.126**	7.526	7.383	7.381	7.692	7.717	7.387	7.752	7.126
Img8	PSNR	32.374	34.871	34.757	34.350	34.166	34.044	**37.366**	34.087	34.086	34.592	34.585	37.366
	Cielab	2.908	2.484	2.541	2.641	2.596	2.667	**1.778**	2.621	2.611	2.572	2.637	1.778
	SSIM	0.852	0.933	0.927	0.917	0.924	0.916	**0.947**	0.924	0.923	0.922	0.914	0.947
	HVS	27.354	27.496	27.491	27.208	27.416	27.960	**32.424**	27.452	27.446	27.414	27.514	32.424
	HVSm	29.174	29.235	29.314	29.137	29.311	29.832	**34.814**	29.321	29.327	29.189	29.283	34.814
	NIQE	10.212	5.660	5.675	5.617	5.763	5.685	**5.208**	5.840	5.844	5.685	5.821	5.208
Img9	PSNR	47.289	**48.493**	48.466	48.315	48.382	43.515	48.447	48.170	48.167	45.608	48.271	48.493
	Cielab	0.504	0.467	0.469	0.476	0.469	0.683	**0.462**	0.479	0.479	0.558	0.481	0.462
	SSIM	0.692	**0.824**	0.820	0.813	0.823	0.706	0.782	0.811	0.810	0.775	0.787	0.824
	HVS	42.747	42.874	42.861	42.752	42.825	40.129	**43.373**	42.808	42.798	41.591	42.868	43.373
	HVSm	44.060	44.121	44.124	44.050	44.106	41.006	**44.671**	44.111	44.106	42.689	44.129	44.671
	NIQE	17.214	8.509	8.517	8.317	**7.794**	8.903	9.033	8.175	8.132	8.716	9.360	7.794
Img10	PSNR	33.614	36.552	35.255	35.922	35.822	35.673	**37.811**	35.769	35.761	36.227	35.731	37.811
	Cielab	2.456	2.007	2.235	2.161	2.105	2.184	**1.577**	2.122	2.115	2.100	2.245	1.577
	SSIM	0.796	**0.920**	0.911	0.899	0.909	0.898	0.908	0.908	0.908	0.906	0.889	0.920
	HVS	29.178	29.394	28.971	28.903	29.114	29.857	**33.852**	29.166	29.137	29.214	29.182	33.852
	HVSm	31.027	31.134	30.863	30.830	31.015	31.790	**36.335**	31.037	31.016	31.006	30.986	36.335
	NIQE	10.494	4.938	5.058	4.962	4.879	4.883	**4.477**	5.029	5.030	4.978	4.968	4.477
Img11	PSNR	34.061	36.764	35.849	36.154	36.046	35.901	**38.583**	35.978	35.975	36.519	36.124	38.583
	Cielab	2.354	1.970	2.167	2.109	2.061	2.134	**1.504**	2.080	2.072	2.045	2.175	1.504
	SSIM	0.802	**0.918**	0.905	0.897	0.907	0.897	0.912	0.906	0.905	0.905	0.888	0.918
	HVS	29.227	29.445	29.129	28.970	29.212	29.898	**34.038**	29.264	29.237	29.297	29.264	34.038
	HVSm	31.027	31.154	30.937	30.860	31.067	31.782	**36.396**	31.091	31.073	31.061	31.005	36.396
	NIQE	10.481	4.675	4.744	4.666	4.719	4.590	**4.340**	4.810	4.806	4.713	4.936	4.340
Img12	PSNR	29.478	31.840	31.702	31.078	31.159	31.106	**34.716**	31.099	31.084	31.540	31.469	34.716
	Cielab	5.113	4.438	4.529	4.882	4.559	4.781	**2.943**	4.629	4.591	4.614	4.754	2.943
	SSIM	0.855	0.926	0.921	0.901	0.920	0.903	**0.952**	0.920	0.919	0.911	0.904	0.952
	HVS	24.528	24.888	24.772	24.272	24.636	25.195	**31.067**	24.682	24.669	24.740	24.753	31.067
	HVSm	26.702	27.007	26.957	26.612	26.870	27.428	**34.567**	26.896	26.889	26.876	26.886	34.567
	NIQE	10.852	7.333	7.411	7.410	7.668	7.563	**7.308**	7.776	7.788	7.432	7.725	7.308
Img13	PSNR	33.709	36.247	36.036	35.565	35.489	35.348	**38.286**	35.423	35.415	35.844	35.837	38.286
	Cielab	2.836	2.388	2.460	2.584	2.510	2.597	**1.745**	2.531	2.527	2.511	2.573	1.745
	SSIM	0.851	0.936	0.929	0.917	0.926	0.918	**0.945**	0.925	0.925	0.923	0.914	0.945
	HVS	29.430	29.817	29.653	29.357	29.513	30.187	**34.190**	29.595	29.575	29.587	29.694	34.190
	HVSm	31.555	31.860	31.823	31.666	31.772	32.446	**37.118**	31.820	31.818	31.693	31.769	37.118
	NIQE	11.325	7.501	7.534	7.419	7.777	7.576	**7.335**	7.804	7.798	7.505	7.637	7.335
Img14	PSNR	38.709	40.728	40.538	40.214	40.077	38.106	**42.036**	40.009	39.990	39.946	40.247	42.036
	Cielab	1.347	1.182	1.216	1.252	1.227	1.485	**1.001**	1.236	1.236	1.268	1.270	1.001
	SSIM	0.835	**0.918**	0.909	0.902	0.909	0.861	0.916	0.908	0.907	0.897	0.888	0.918
	HVS	33.574	33.793	33.650	33.440	33.487	33.657	**36.198**	33.564	33.515	33.414	33.681	36.198
	HVSm	35.365	35.514	35.481	35.326	35.412	35.363	**37.968**	35.453	35.431	35.130	35.461	37.968
	NIQE	11.303	5.796	5.735	5.641	5.843	5.869	**5.597**	5.954	5.978	5.831	6.255	5.597
Img15	PSNR	36.605	39.054	38.857	38.518	38.352	37.543	**40.074**	38.280	38.275	38.421	38.583	40.074
	Cielab	1.755	1.500	1.544	1.598	1.569	1.694	**1.255**	1.580	1.578	1.590	1.616	1.255
	SSIM	0.824	**0.921**	0.912	0.903	0.910	0.891	0.913	0.909	0.908	0.904	0.891	0.921
	HVS	31.809	32.053	31.894	31.674	31.793	32.433	**34.010**	31.847	31.826	31.728	31.945	34.010
	HVSm	33.612	33.769	33.715	33.560	33.696	34.331	**35.773**	33.722	33.714	33.461	33.708	35.773
	NIQE	10.822	5.290	5.270	5.192	5.305	5.372	**5.172**	5.424	5.425	5.318	5.631	5.172
Img16	PSNR	35.335	37.970	37.798	37.331	37.242	36.801	**39.720**	37.164	37.159	37.406	37.560	39.720
	Cielab	2.057	1.745	1.788	1.875	1.816	1.950	**1.319**	1.834	1.829	1.867	1.871	1.319
	SSIM	0.833	0.923	0.917	0.904	0.914	0.897	**0.931**	0.913	0.912	0.905	0.899	0.931
	HVS	30.547	30.864	30.704	30.329	30.583	31.157	**35.404**	30.649	30.630	30.620	30.744	35.404
	HVSm	32.564	32.825	32.762	32.499	32.718	33.266	**37.986**	32.762	32.750	32.610	32.732	37.986
	NIQE	11.633	6.670	6.695	6.665	**6.629**	6.658	6.650	6.807	6.788	6.711	7.047	6.629
Img17	PSNR	38.138	40.186	40.091	39.750	39.612	39.345	**41.737**	39.522	39.521	39.628	39.881	41.737
	Cielab	1.372	1.206	1.230	1.274	1.247	1.302	**0.997**	1.258	1.257	1.265	1.281	0.997
	SSIM	0.836	0.915	0.910	0.900	0.908	0.893	**0.920**	0.907	0.906	0.900	0.893	0.920
	HVS	33.267	33.383	33.428	33.203	33.378	33.663	**35.719**	33.420	33.412	33.127	33.430	35.719
	HVSm	35.114	35.166	35.268	35.139	35.289	35.490	**37.648**	35.319	35.314	34.855	35.239	37.648
	NIQE	11.888	6.002	5.971	**5.773**	5.999	6.094	5.988	6.074	6.080	6.089	6.471	5.773
Img18	PSNR	34.632	36.963	36.862	36.414	36.328	36.249	**38.906**	36.251	36.254	36.645	36.653	38.906
	Cielab	2.313	1.982	2.018	2.118	2.062	2.125	**1.472**	2.082	2.076	2.059	2.105	1.472
	SSIM	0.835	0.925	0.921	0.908	0.917	0.908	**0.931**	0.917	0.916	0.914	0.904	0.931
	HVS	29.839	30.115	30.087	29.783	30.058	30.359	**33.498**	30.114	30.106	29.939	30.067	33.498
	HVSm	31.785	31.983	32.010	31.831	32.057	32.300	**35.886**	32.096	32.093	31.799	31.954	35.886
	NIQE	10.642	5.604	5.629	5.541	5.711	5.634	**5.499**	5.836	5.828	5.643	5.891	5.499
Img19	PSNR	35.442	37.824	37.720	37.375	37.213	36.919	**39.716**	37.146	37.141	37.447	37.512	39.716
	Cielab	1.984	1.700	1.735	1.796	1.770	1.842	**1.282**	1.783	1.781	1.769	1.806	1.282
	SSIM	0.834	0.924	0.919	0.908	0.916	0.903	**0.931**	0.915	0.914	0.911	0.902	0.931
	HVS	30.611	30.805	30.774	30.541	30.731	31.158	**34.282**	30.776	30.763	30.624	30.786	34.282
	HVSm	32.314	32.423	32.457	32.315	32.487	32.880	**36.404**	32.512	32.505	32.251	32.431	36.404
	NIQE	10.529	4.922	4.913	4.853	4.825	4.929	**4.781**	5.007	5.019	4.956	5.270	4.781
Img20	PSNR	36.051	38.362	38.259	37.838	37.705	37.752	**39.983**	37.636	37.626	38.169	38.113	39.983
	Cielab	1.981	1.707	1.736	1.816	1.777	1.817	**1.331**	1.793	1.789	1.760	1.798	1.331
	SSIM	0.823	0.919	0.915	0.902	0.911	0.905	**0.919**	0.910	0.910	0.910	0.900	0.919
	HVS	31.334	31.601	31.533	31.231	31.465	31.847	**34.316**	31.512	31.496	31.467	31.543	34.316
	HVSm	33.188	33.374	33.357	33.164	33.357	33.711	**36.334**	33.387	33.375	33.260	33.331	36.334
	NIQE	10.523	4.872	4.885	4.865	4.740	4.857	**4.639**	4.955	4.985	4.891	5.101	4.639
Average	PSNR	36.563	38.802	38.597	38.335	38.214	37.225	**40.344**	38.117	38.113	37.937	38.467	40.344
	Cielab	2.111	1.813	1.863	1.931	1.880	1.994	**1.371**	1.901	1.893	1.906	1.929	1.371

SSIM	0.817	**0.911**	0.906	0.896	0.904	0.876	0.908	0.901	0.901	0.890	0.888	0.911
HVS	31.803	32.016	31.944	31.732	31.904	31.943	**35.259**	31.941	31.928	31.688	31.966	35.259
HVSm	33.594	33.731	33.725	33.600	33.744	33.705	**37.459**	33.764	33.759	33.396	33.707	37.459
NIQE	11.843	6.205	6.197	6.126	6.161	6.478	**6.110**	6.282	6.281	6.384	6.579	**6.110**

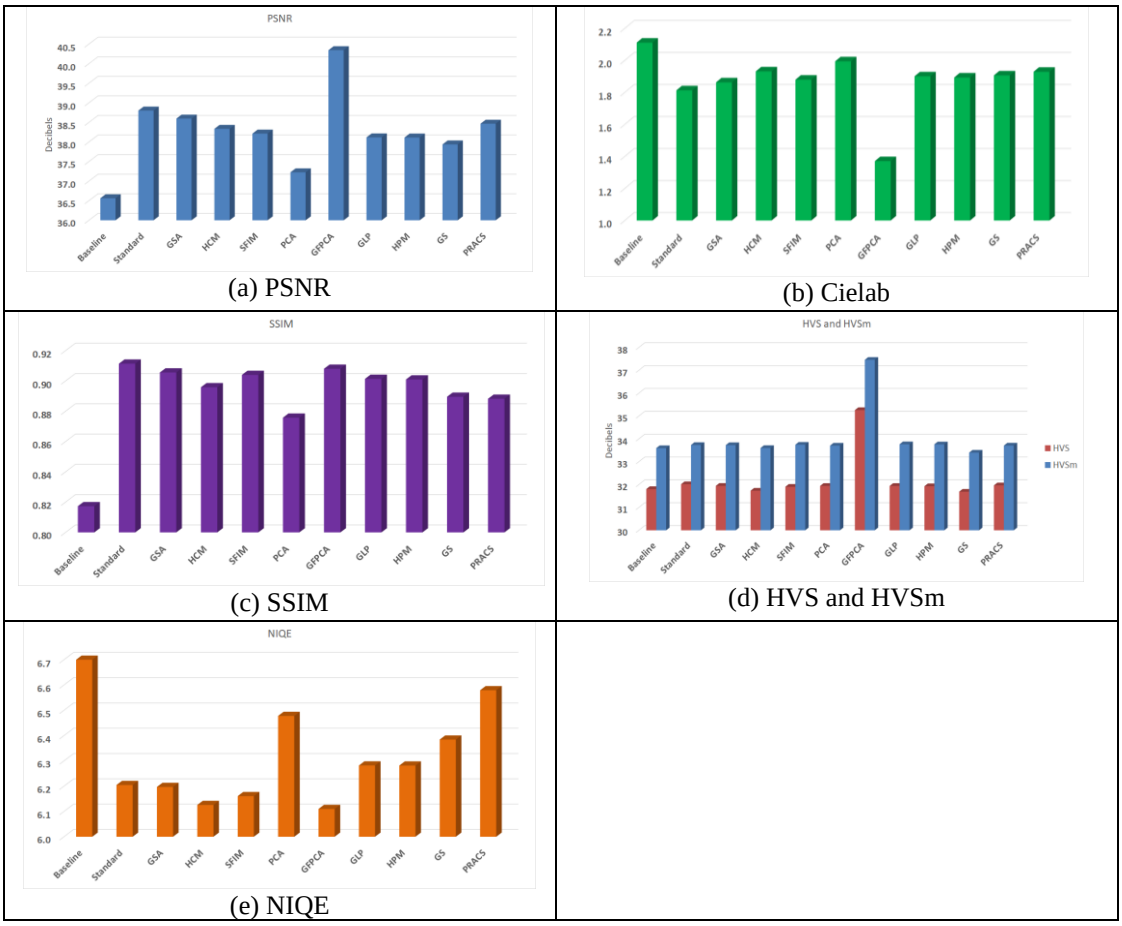

(a) PSNR (b) Cielab

(c) SSIM (d) HVS and HVSm

(e) NIQE

Figure 11. Averaged performance metrics for demosaicing results of right Mastcam images.

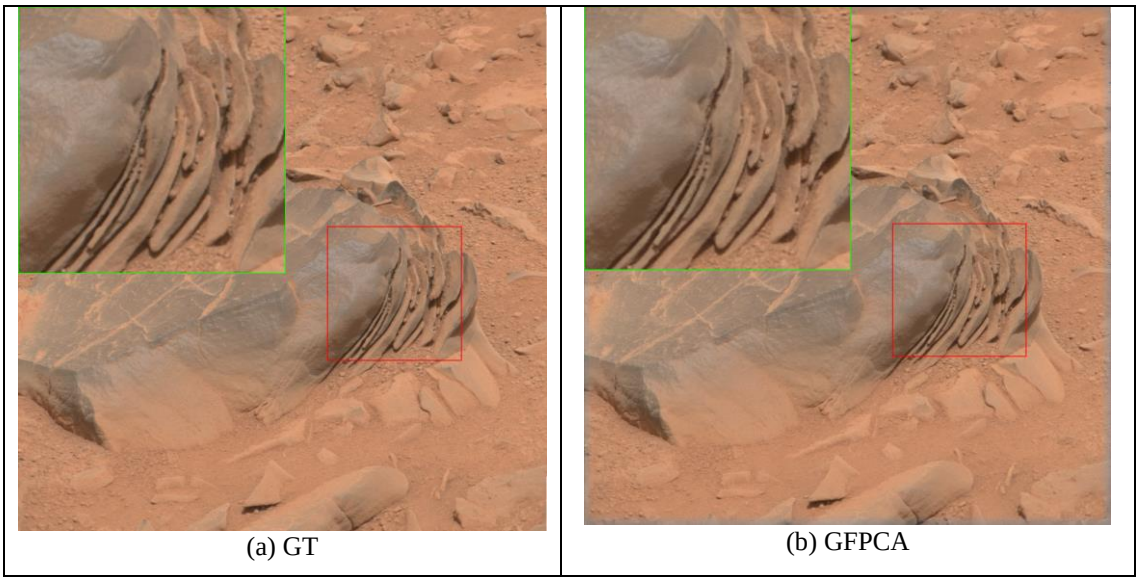

(a) GT (b) GFPCA

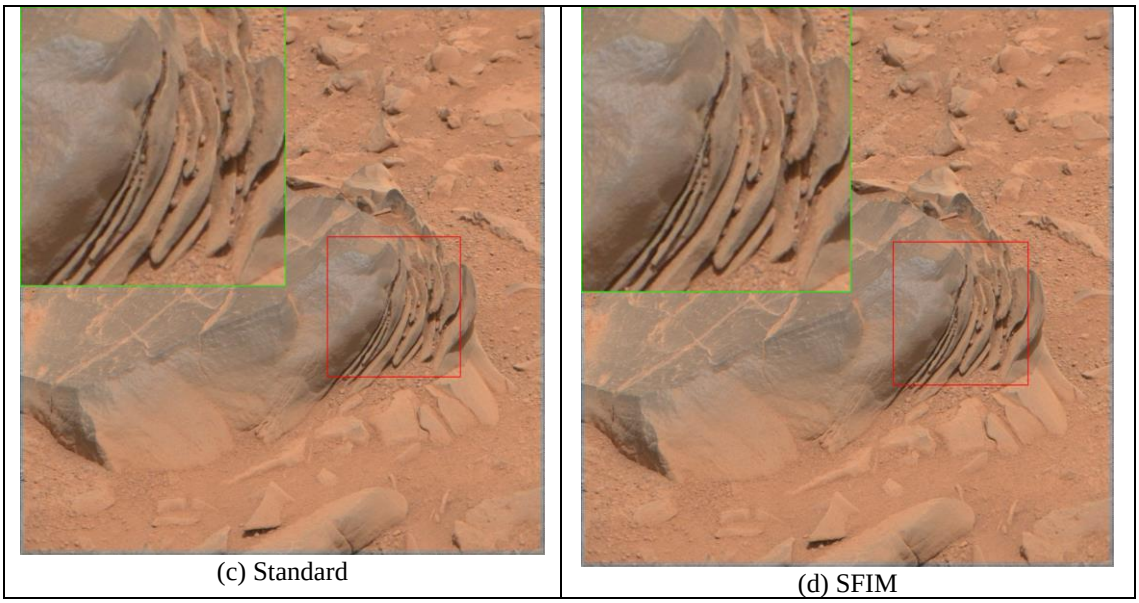

(c) Standard (d) SFIM

Figure 12. Visual comparison of the ground truth and selected demosaiced images for right Mastcam.

4. CONCLUSIONS

In this paper, we first review the Mastcam and the demosaicing problem for Mastcam images. Earlier results of improving the Mastcam image demosaicing using CFA 1.0 was reviewed. We then summarize our investigation of a new CFA for demosaicing Mastcam images. Our goal is to determine whether or not the new CFA can work well under normal lighting conditions. Based on the experimental results, CFA 3.0 can work quite well in normal lighting conditions. In the future, we will continue to investigate CFA 3.0 for actual low lighting Mastcam images, which will need to be searched amongst close to one million images in the image archive.

ACKNOWLEDGEMENTS

This research was supported in part by NASA Jet Propulsion Laboratory under contract 80NSSC17C0035. The views, opinions and/or findings expressed are those of the author and should not be interpreted as representing the official views or policies of NASA or the U.S. Government.

REFERENCES

[1] B. Ayhan, C. Kwan, and S. Vance, “On the Use of a Linear Spectral Unmixing Technique for Concentration Estimation of APXS Spectrum,” J. Multidisciplinary Engineering Science and Technology, Volume 2, Issue 9, September, 2015.

[2] W. Wang, S. Li, H. Qi, B. Ayhan, C. Kwan, and S. Vance, “Revisiting the Preprocessing Procedures for Elemental Concentration Estimation based on CHEMCAM LIBS on MARS Rover,” 6th Workshop on Hyperspectral Image and Signal Processing: Evolution in Remote Sensing (WHISPERS), Lausanne, Switzerland, June 24-27, 2014.

[3] J. F. Bell et al., “The Mars Science Laboratory Curiosity Rover Mast Camera (Mastcam) Instruments: Pre-Flight and In-Flight Calibration, Validation, and Data Archiving,” AGU journal Earth and Space Science, 2017.

[4] https://www.forbes.com/sites/trevornace/2019/06/25/nasas-mars-rover-just-detected-an-unusual-spike-in-greenhouse-gas-emissions/#512e18922f0f

[5] B. Ayhan and C. Kwan, “Mastcam Image Resolution Enhancement with Application to Disparity Map Generation for Stereo Images with Different Resolutions,” Sensors, August 12, 2019.

[6] C. Kwan, B. Chou, and B. Ayhan, "Enhancing Stereo Image Formation and Depth Map Estimation for Mastcam Images," IEEE Ubiquitous Computing, Electronics & Mobile Communication Conference, New York City, November 2018.
[7] B. Ayhan, M. Dao, C. Kwan, H. Chen, J. F. Bell III, and R. Kidd, "A novel utilization of image registration techniques to process Mastcam images in Mars rover with applications to image fusion, pixel clustering, and anomaly detection," IEEE Journal of Selected Topics in Applied Earth Observations and Remote Sensing, Vol. 10, Issue: 10, Pages: 4553 - 4564, 2017.
[8] C. Kwan, J. Larkin, B. Budavari, and B. Chou, "Compression algorithm selection for multispectral Mastcam images," Signal & Image Processing: An International Journal (SIPIJ), February 28, 2019.
[9] https://www.msss.com/msl/mastcam/MastCam_description.html
[10] B. Bayer, "Color imaging array," US Patent 3,971,065, 1976.
[11] H. S. Malvar, L.-W. He, and R. Cutler, "High-quality linear interpolation for demosaciking of color images," In Processing of the IEEE International Conference on Acoustics, Speech, and Signal Processing, Montreal, Québec, Canada, pp. 485–488, 17–21 May 2004.
[12] L. Zhang and X. Wu, "Color demosaicking via directional linear minimum mean square-error estimation," IEEE Trans. Image Process, vol. 14, pp. 2167–2178, 2005.
[13] J. Hamilton and J. Compton, "Processing color and panchromatic pixels," U.S. Patent 20070024879A1, 2007.
[14] C. Kwan and B. Chou, "Further improvement of debayering performance of RGBW color filter arrays using deep learning and pansharpening techniques," J. Imaging, 5(8), 68, 2019.
[15] T. Kijima, H. Nakamura, J. T. Compton, J. F. Hamilton, and T. E. DeWeese, "Image sensor with improved light sensitivity," U.S. Patent 0 268 533, Nov., 2007.
[16] C. Zhang, Y. Li, J. Wang, and P. Hao, "Universal demosaicking of color filter arrays," IEEE Trans. Image Processing, 25, 2016.
[17] L. Condat, "A generic variational approach for demosaicking from an arbitrary color filter array," Proceedings of the IEEE Int. Conf. Image Process. (ICIP), Cairo, Egypt, 1625–1628, Nov. 2009.
[18] D. Menon and G. Calvagno, "Regularization approaches to demosaicking," IEEE Trans. Image Process., 18, 2209–2220, 2009.
[19] C. Kwan, J. Larkin, and B. Ayhan, "Demosaicing of CFA 3.0 with Application to Low Lighting Images," Sensors, June 17, 2020.
[20] C. Kwan and J. Larkin, "Demosaicing of Bayer and CFA2.0 Patterns for Low Lighting Images," Electronics, 8(12), 1444, December 1, 2019.
[21] L. Zhang, X. Wu, A. Buades, and X. Li, "Color demosaicking by local directional interpolation and nonlocal adaptive thresholding," J. Electron. Imaging, 20, 2011.
[22] W. Lu and Y. P. Tan, "Color filter array demosaicking: New method and performance measures," IEEE Trans. on Image Processing, 12, 1194–1210, 2003.
[23] E. Dubois, "Frequency-domain methods for demosaicking of Bayer-sampled color images," IEEE Signal Proc. Letters, 12, 847–850, 2005.
[24] B. Gunturk, Y. Altunbasak, and R. M. Mersereau, "Color plane interpolation using alternating projections," IEEE Transactions on Image Processing, 11, 997–1013, 2002.
[25] X. Wu and N. Zhang, "Primary-consistent soft-decision color demosaicking for digital cameras," IEEE Trans. on Image Processing, 13, 1263-1274, 2004.
[26] C. Kwan, B. Chou, L. M. Kwan, J. Larkin, B. Ayhan, J. F. Bell, and H. Kerner, "Demosaicking enhancement using pixel-level fusion," Journal of Signal, Image, and Video Processing, 12, 749, 2018.
[27] J. Bednar and T. Watt, "Alpha-trimmed means and their relationship to median filters," IEEE Trans. Acoustics, Speech, and Signal Processing, 32, 145-153, 1984.
[28] M. Gharbi, G. Chaurasia, S. Paris, and F. Durand, "Deep joint demosaicking and denoising," ACM Trans. Graph, 35, 2016.
[29] G. Vivone, et al., "A Critical Comparison Among Pansharpening Algorithms," IEEE Trans. Geoscience and Remote Sensing, 53(5), 2015.
[30] J. G. Liu, "Smoothing filter based intensity modulation: A spectral preserve image fusion technique for improving spatial details," Int. J. Remote Sens., 21, 18, 2000.
[31] B. Aiazzi, et al., "MTF-tailored multiscale fusion of high-resolution MS and pan imagery," Photogramm. Eng. Remote Sens., 72(5), pp. 591–596, 2006.
[32] G. Vivone, et al., "Contrast and error-based fusion schemes for multispectral image pansharpening," IEEE Trans. Geosci. Remote Sensing Lett., 11(5), pp. 930–934, 2014.

[33] C. Laben amd B. Brower, "Process for enhancing the spatial resolution of multispectral imagery using pan-sharpening," U.S. Patent 6 011 875, Jan. 4, 2000.
[34] B. Aiazzi, et al., "Improving component substitution pansharpening through multivariate regression of MS+pan data," IEEE Trans. Geosci. Remote Sensing, 45(10), pp. 3230–3239, 2007.
[35] W. Liao, et al., "Processing of multiresolution thermal hyperspectral and digital color data: Outcome of the 2014 IEEE GRSS data fusion contest," IEEE J. Select. Top. Appl. Earth Observ. Remote Sensing, 8, 6, 2015.
[36] J. Choi, et al., "A new adaptive component-substitution based satellite image fusion by using partial replacement," IEEE Trans. Geosci. Remote Sens., 49, 1, 2011.
[37] J. Zhou, C. Kwan, and B. Budavari, "Hyperspectral image super-resolution: A hybrid color mapping approach," Journal of Applied Remote Sensing, 10, 3, article 035024, 2016.
[38] C. Kwan, J. H. Choi, S. Chan, J. Zhou, and B. Budavai, "Resolution Enhancement for Hyperspectral Images: A Super-Resolution and Fusion Approach," IEEE International Conference on Acoustics, Speech, and Signal Processing, pp. 6180 – 6184, New Orleans, 2017.
[39] C. Kwan, B. Budavari, F. Gao, and X. Zhu, "A Hybrid Color Mapping Approach to Fusing MODIS and Landsat Images for Forward Prediction," Remote Sensing, 10 (4), 520, 2018.
[40] C. Kwan, B. Ayhan, and B. Budavari, "Fusion of THEMIS and TES for Accurate Mars Surface Characterization," IEEE International Geoscience and Remote Sensing Symposium, pp. 3381-3384, 2017.
[41] C. Kwan, X. Zhu, F. Gao, B. Chou, D. Perez, J. Li, Y. Shen, and K. Koperski, "Assessment of Spatiotemporal Fusion Algorithms for Planet and Worldview Images," Sensors, 18, 1051, 2018.
[42] SSIM. Available online: https://en.wikipedia.org/wiki/Structural_similarity. (Accessed on 26 April 2019).
[43] K. Egiazarian, J. Astola, N. Ponomarenko, V. Lukin, F. Battisti, and M. Carli, "New full quality metrics based on HVS," In Proceedings of the Second International Workshop on Video Processing and Quality Metrics, Scottsdale, AZ, USA, 22–24 January 2006.
[44] N. Ponomarenko, F. Silvestri, K. Egiazarian, M. Carli, J. Astola, and V. Lukin, "On between-coefficient contrast masking of DCT basis functions," In Proceedings of the Third International Workshop on Video Processing and Quality Metrics for Consumer Electronics VPQM-07, Scottsdale, AZ, USA, 25–26 January 2007.
[45] X. Zhang and B. A. Wandell, "A spatial extension of cielab for digital color image reproduction," SID Journal, 1997.
[46] C. Kwan, B. Budavari, A. Bovik, and G. Marchisio, "Blind Quality Assessment of Fused WorldView-3 Images by Using the Combinations of Pansharpening and Hypersharpening Paradigms," IEEE Geoscience and Remote Sensing Letters, Vol.14, no. 10, pp. 1835 - 1839, 2017.
[47] A. Mittal, R. Soundararajan and A. C. Bovik, "Making a Completely Blind Image Quality Analyzer ", IEEE Signal processing Letters, vol. 22, no. 3, pp. 209-212, March 2013.
[48] C. Kwan and B. Chou, "A comparative study of conventional and deep learning approaches for demosaicing Mastcam images," Proc. SPIE. 11018, Signal Processing, Sensor/Information Fusion, and Target Recognition XXVIII (Conference SI219), April 2019.
[49] C. Kwan, B. Chou, and J. F. Bell, "Comparison of deep learning and conventional demosaicing algorithms for Mastcam images," Electronics, (2019).

AUTHORS

Chiman Kwan received his Ph.D. degree in electrical engineering from the University of Texas at Arlington in 1993. He has 15 patents, 65 invention disclosures, 370 technical papers in journals and conferences, and 550 technical reports. Over the past 25 years, he has been the PI/Program Manager of over 120 diverse projects with total funding exceeding 36 million dollars. He is also the founder and Chief Technology Officer of Signal Processing, Inc. and Applied Research LLC. He received numerous awards from IEEE, NASA, and some other agencies.

Jude Larkin received his B.S. in Computer Science from Franciscan University of Steubenville in 2015. He is a software engineer at ARLLC. He has been involved in diverse projects, including mission planning for UAVs, image fusion, image demosaicing, and remote sensing.